JOC The Journal of Organic Chemistry

pubs.acs.org/joc Article

Mechanisms of Formation and Rearrangement of Benziodoxole-Based CF_3 and SCF_3 Transfer Reagents

Oriana Brea, Kalman J. Szabo,* and Fahmi Himo*

Cite This: J. Org. Chem. 2020, 85, 15577−15585 Read Online

ACCESS | Metrics & More | Article Recommendations | Supporting Information

ABSTRACT: Togni's benziodoxole-based reagents are widely used in trifluoromethylation reactions. It has been established that the kinetically stable hypervalent iodine form (I−CF_3) of the reagents is thermodynamically less stable than its acyclic ether isomer (O−CF_3). On the other hand, the trifluoromethylthio analogue exists in the thermodynamically stable thioperoxide form (O−SCF_3), and the hypervalent form (I−SCF_3) has been elusive. Despite the importance of these reagents, very little is known about the reaction mechanisms of their syntheses, which has hampered the development of new reagents of the same family. Herein, we use density functional theory calculations to understand the reasons for the divergent behaviors between the CF_3 and SCF_3 reagents. We demonstrate that they follow different mechanisms of formation and that the metals involved in the syntheses (potassium in the case of the trifluoromethyl reagent and silver in the trifluoromethylthio analogue) play key roles in the mechanisms and greatly influence the possibility of their rearrangements from the hypervalent (I−CF_3, I−SCF_3) to the corresponding ether-type form (O−CF_3, O−SCF_3).

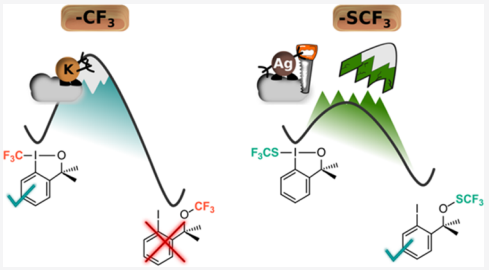

1. INTRODUCTION

Organofluorine compounds are widely used as pharmaceutical[1] and agrochemical products[2] and in medical diagnostics.[3] One of five commercial drugs and one of three new agrochemical substances contain at least one C−F bond.[1,4] One of the main reasons for the widespread application of these compounds is their high metabolic stability, which, among other things, leads to smaller doses necessary to achieve the desired bioactivity compared to the nonfluorinated analogues.[1] However, organofluorine compounds have different chemical and metabolic stabilities depending on the chemical environment of the C−F bond. Some of the most stable aliphatic species involve trifluoromethyl/perfluoroalkyl and trifluoromethylthiol derivatives.

The large demand for fluorinated compounds, in particular fluoroalkylated ones containing CF_3 and SCF_3 groups, has stimulated the development of new synthetic methodologies for the selective preparation of fairly complex organofluorine species.[5−7] In this context, one of the most important developments in the last 10−15 years has been the appearance of new reagents that can be employed for synthesis of organofluorines with high levels of selectivity. An important example of these reagents is Togni's hypervalent iodine reagent **1** (Scheme 1), which can be used for the transfer of a trifluoromethyl group to a wide range of organic substrates.[5−7] Although the Togni reagent was first reported in 2006,[7] surprisingly few hypervalent iodine-based benziodoxole reagents have been reported that are suitable for the transfer of other fluorinated functional groups. Some of the few examples are fluorine and perfluoroalkyl transfer reagents **2**[8−10] and **3**,[11] as well as the CF_2-SO_2Ph analogue **4**.[12] On the other hand, the synthesis of benziodoxole-based SCF_3 transfer reagent **5** was unsuccessful and yielded the thioperoxide isomer **7**.[13,14] Most probably, many failed attempts for the synthesis of reagents with hypervalent iodine bound $-CF_2R$ (R ≠ F, CF_2R, CF_2SO_2Ph) have not been reported.

Schaefer and co-workers[15] pointed out that many hypervalent iodine-based reagents, such as **1** and **5**, are thermodynamically much less stable than their corresponding ether-type analogues, such as **6** and **7**, which could explain the synthetic difficulties in accessing the hypervalent iodine reagents. Yet, **1** can be easily prepared, while **5** has never been observed. This suggests that certain benziodoxole-based reagents, such as **1**, are kinetically stable, while others rearrange to the thermodynamically most stable isomer or never form under the applied conditions of the synthesis. One may therefore pose the following question: What is the reason for the high kinetic stability of the hypervalent form of **1** as compared to **5**? The answer to this question and the details involved in the mechanism of the synthesis of this class of reagents would certainly be highly valuable in the design of new fluoroalkyl group-based hypervalent benziodoxole reagents for

Received: September 28, 2020
Published: November 17, 2020

https://dx.doi.org/10.1021/acs.joc.0c02306
J. Org. Chem. 2020, 85, 15577−15585

Scheme 1. Hypervalent Iodine-Based Benziodoxole Reagents for the Synthesis of Organofluorine Compounds (1−4) and Some of the Thermodynamically Stable Isomers (6 and 7)

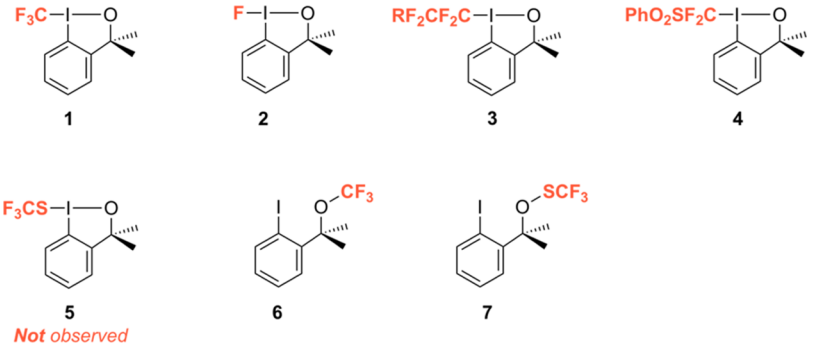

selective synthesis of new organofluorine compounds for the pharmaceutical industry and medical diagnostics.

To this end, we have, in the present work, performed density functional theory (DFT) calculations to elucidate the mechanism of the formation of the Togni reagent **1** from the reaction of fluoro-benziodoxole **2** with the Ruppert−Prakash reagent **8** in the presence of KF (the second part of reaction I in Scheme 2).[9] Quite surprisingly, knowledge about the mechanism of the synthesis of this important reagent has been missing. For comparison, we also studied the mechanism of the attempted synthesis of the trifluoromethylthio analogue **5** from the reaction of chloro-benziodoxole **9** with $AgSCF_3$ **10** (reaction II in Scheme 2).[13,14] In both cases, we studied the rearrangement possibilities of the hypervalent iodine species to the corresponding thermodynamically stable ether-type isomers.

Scheme 2. Syntheses of Benziodoxole-Based CF_3 (1, Togni Reagent) and SCF_3 (7) Transfer Reagents Investigated in the Current Study

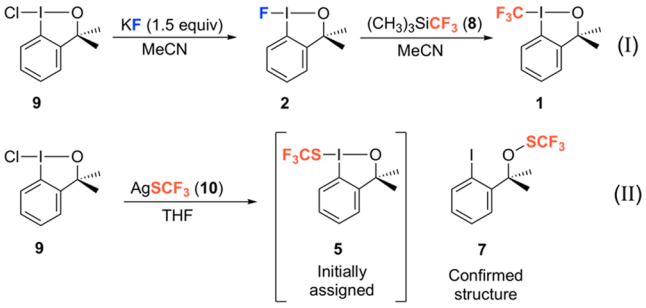

2. RESULTS AND DISCUSSION

2.1. Mechanism of the Synthesis of the Togni Reagent. The standard procedure for the synthesis of the Togni reagent **1** is shown in Scheme 2.[9] It starts with chloro-benziodoxole **9**, which is converted to fluoro-benziodoxole **2**. Subsequently, **2** is reacted with the Ruppert−Prakash reagent **8** in the presence of potassium fluoride to obtain **1**. We focus here on the second part of the synthesis, i.e., the conversion of **2** with **8** and KF. We considered two main possibilities under these conditions. Conversion of **2** to Togni reagent **1** and an alternative pathway involving the formation of the thermodynamically more stable ether form **6**. In connection with these studies, we also investigated the possible formation of **6** from **1** under the above reaction conditions.

We start the computational investigation by examining the possible adducts that may form from various precursors present in the reaction mixture, i.e., **2**, **8**, and KF. The calculations show that the most stable complex is formed between **2** and KF (called **2·KF**), in which the fluoride is associated with the iodine center and the potassium with the oxygen side, as displayed in Scheme 3 (optimized geometries of **2·KF** and other possible complexes with higher energies are given in the Supporting Information).

Scheme 3. Proposed Mechanism of the Synthesis of the Togni Reagent 1 as Obtained from the Current DFT Calculations

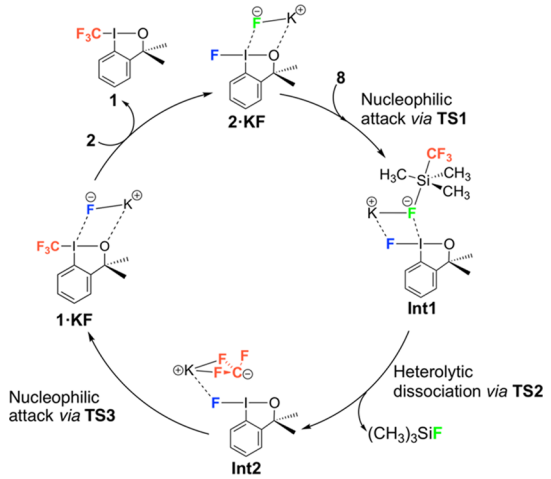

From **2·KF**, the reaction mechanism obtained on the basis of the current DFT calculations is shown in Scheme 3, and the associated energy profile is given in Figure 1. Optimized structures of key transition states (TSs) and intermediates are depicted in Figure 2, while other geometries are supplied in the Supporting Information. The first step of the reaction is the nucleophilic attack of the fluoride of KF on the silicon center of **8** via **TS1**. This step has a calculated barrier of 10.1 kcal/mol relative to **2·KF**. In order for the nucleophilic attack to take place, the KF has to change its orientation relative to **1** such that the potassium points in the direction of the fluorine. This structure is called **2·KF′** and is 3.6 kcal/mol higher than **2·KF** (Figure 1). At **TS1**, the F−Si bond distance is 2.72 Å, and the fluoride interacts also with the iodine with a distance of 2.49 Å (Figure 2). The nucleophilic attack results in **Int1**, which is 3.7 kcal/mol higher than **2·KF** and which involves a hypervalent silicon center, with F−Si and Si−CF_3 bond distances of 1.84 and 2.01 Å, respectively (Figure 2). The negative charge in **Int1** is

https://dx.doi.org/10.1021/acs.joc.0c02306
J. Org. Chem. 2020, 85, 15577−15585

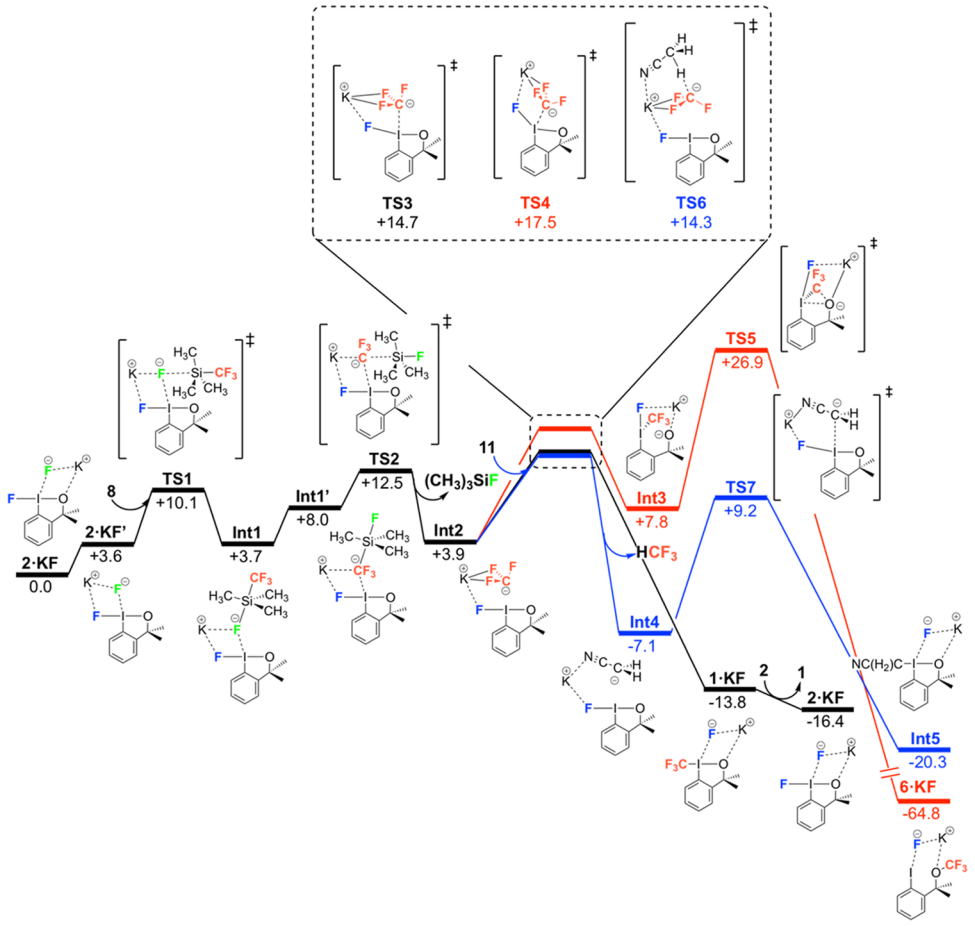

Figure 1. Calculated free energy profile (kcal/mol) for reaction I (black), the formation of the ether product (red), and the formation of a potential side product by reaction with an acetonitrile solvent molecule **11** (blue).

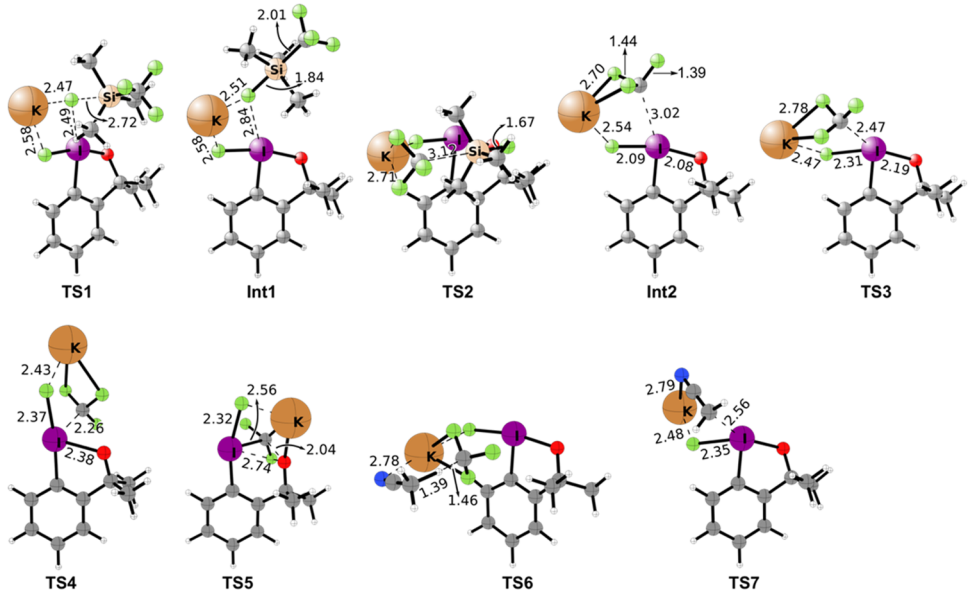

Figure 2. Optimized geometries of selected transition states and intermediates involved in the synthesis of the Togni reagent. Distances are given in Ångström (Å).

distributed over the fluorine and trifluoromethyl group (see calculated charge distribution in the Supporting Information).

The next step involves a heterolytic dissociation of the Si–CF_3 bond. Direct dissociation at **Int1** has a barrier of 18.2 kcal/mol relative to **2·KF**. Instead, we found that a prior reorientation of the anionic moiety in **Int1**, such that the CF_3 group is positioned toward the potassium (**Int1′** in Figure 1), leads to a lower barrier for the (heterolytic) Si–CF_3 bond dissociation.

https://dx.doi.org/10.1021/acs.joc.0c02306
J. Org. Chem. 2020, 85, 15577−15585

Such a reorientation is not associated with a high energy (see the Supporting Information), and the barrier for the Si−C bond cleavage from **Int1′** via **TS2** is calculated to be 12.5 kcal/mol relative to **2·KF**. This step releases the trimethylfluorosilane $(CH_3)_3SiF$ side product and generates intermediate **Int2**.[16] In **Int2**, the CF_3 anion interacts bidentately with the potassium cation (Figure 2). The lone pair of the CF_3^- moiety in **Int2** points in the direction of the iodine (see the Supporting Information), in anticipation of nucleophilic attack at the hypervalent iodine, which then takes place with the simultaneous loss of fluorine from the iodine to yield Togni reagent **1** in complex with KF (**1·KF**). This concerted step occurs through **TS3**, with a barrier of 14.7 kcal/mol relative to **2·KF**, and constitutes thus the highest barrier of the reaction. At **TS3**, the I−CF_3 bond distance is shortened to 2.47 Å, while the I−F distance is elongated to 2.31 Å.

According to this mechanistic proposal, KF plays the role of not only an initiator in the reaction but also of a catalyst, donating a fluorine to the Ruppert−Prakash reagent **8** in the first step and receiving back a fluorine from fluoro-benziodoxole reagent **2** (Scheme 3). To complete the cycle, an exchange between **1** by **2** takes place to regenerate **2·KF**, a step that is exergonic by 2.6 kcal/mol. The entire cycle is thus calculated to be exergonic by 16.4 kcal/mol.

The initial steps leading to the formation of the trifluoromethyl anion can be compared to the results of a computational study of a similar reaction in the context of the activation of the Ruppert−Prakash reagent with KCl as an initiator.[17] In that case, no distinct hypervalent silyl intermediate corresponding to **Int1** could be located, and the formation of CF_3^- was found to take place through a 4-membered TS with concerted Si−Cl bond formation and Si−CF_3 bond cleavage.[17]

Int2, which involves the potassium-bound CF_3 anion, is a key intermediate in the reaction. CF_3^- is of course an excellent nucleophile that is able to displace the substituent on the hypervalent iodine. It is also a strong base (vide infra). It is known that CF_3^- can readily undergo α-elimination by cleavage of one of the C−F bonds to give CF_2 carbene. A similar reaction may also take place with some metal complexes, such as in Cu−CF_3,[18] strongly limiting the synthetic scope of CF_3^--mediated nucleophilic trifluoromethylation reactions. The current mechanistic results show that coordination to the potassium cation effectively stabilizes CF_3^- and prevents the formation of CF_2 carbene, allowing thus the formation of the Togni product **1**. The calculations show that the CF_3^- intermediate can also form in the absence of **2**, i.e., in the reaction between the Ruppert−Prakash reagent and KF (see the Supporting Information for details).

It is interesting here to compare the mechanism shown in Scheme 3 with the one obtained by Schoenebeck and co-workers for the transmetalation of $[Pd^{II}]$−F complexes with the Ruppert−Prakash reagent **8** to yield $[Pd^{II}]$−CF_3 intermediates.[19] In that case, the calculations showed that the reaction proceeds through a short-lived Pd-difluorocarbene intermediate.

We now turn to the question of why the trifluoromethyl ether isomer of **1**, i.e., compound **6**, is not observed experimentally under the above reaction conditions despite the fact that it is thermodynamically much more favored over the hypervalent iodine form, by more than 50 kcal/mol.[15,20] As mentioned above, Schaefer and co-workers hypothesized that the synthetic pathway yields the hypervalent form, which is then kinetically blocked from converting to the ether form.[15] Very similar to their results, we find that the direct isomerization of **1** to **6** is associated with a very high barrier, >45 kcal/mol (see the Supporting Information). We have also considered whether the potassium is able to catalyze the isomerization, but the involvement of **KF** was found to lower the barrier by only ca. 5 kcal/mol, which is not sufficient for observing **6** (see the Supporting Information).

One can envision that the formation of **6** is achieved prior to the formation of **1**, i.e., starting from **Int2**. The first step from this intermediate would be through **TS4**, in which a nucleophilic attack of CF_3^- at the iodine center takes place concertedly with the cleavage of the I−O bond to yield the oxyanion **Int3** (Figure 1). The calculated energy barrier for this step is +17.5 kcal/mol, and **Int3**, despite being an oxygen-based anion, is 3.9 kcal/mol higher than **Int2**. As discussed above, the interaction of the CF_3 anion with the potassium cation helps stabilizing this intermediate. Also, the F−I−C hypervalent bond in **Int3** is less stable than the F−I−O in **Int2**, which involves two electronegative atoms.

Next, **6** can be obtained from **Int3** through **TS5**, which is an electrophilic trifluoromethylation of the oxyanion, by a dissociation of the F−I and I−CF_3 bonds and the formation of the O−CF_3 bond (Figure 2). However, the energy barrier associated with this step was found to be high, 26.9 kcal/mol relative to **2·KF**, i.e., 12.2 kcal/mol higher than the barrier for the formation of **1** through **TS3**. Thus, these results show that the high barrier associated with **TS5** kinetically blocks the formation of **6**, explaining why it is not observed experimentally under the above conditions for the synthesis of **1**.

Interestingly, during the course of our investigations, we also discovered another reaction that can take place from **Int2**, namely, the CF_3^- anion can act as a base, abstracting a proton from an acetonitrile solvent molecule **11** (Figure 1). Such reactivity has been reported previously for the reaction in the absence of **2**.[21,22] The barrier for this proton transfer (**TS6**) is calculated to be 14.3 kcal/mol, which is very close to the barrier found for the formation of **1** (**TS3**, 14.7 kcal/mol).[23] From the resulting **Int4**, a concerted nucleophilic attack and fluoride loss through **TS7** can take place to yield the hypervalent iodine **Int5**. Geometrically, this transition state resembles **TS3**, and the calculated barrier is 16.3 kcal/mol relative to **Int4**. **Int5**, which is 6.5 kcal/mol more stable than Togni reagent **1·KF**, might of course rearrange and react further to yield other side products. This has not been studied explicitly here. The existence of this competitive mechanistic path might contribute to lowering the yields obtained in the synthesis of **1** in acetonitrile.

To summarize the results of this section, the calculations provide detailed insights into the mechanism of the formation of **1**, which is demonstrated to be kinetically favored over the formation of its ether isomer **6**. A plausible competitive pathway that involves the reaction with an acetonitrile solvent molecule is also shown to be possible.

2.2. Mechanism of Synthesis of 7. Having established the mechanism for the synthesis of the Togni reagent, we now turn our attention to the mechanism of the synthesis of **7** and the reasons why the thioperoxide isomer is obtained in this case and not the hypervalent iodine form **5**. In the synthesis of **7**, $AgSCF_3$ **10** is employed as the source of SCF_3 (Scheme 2),[13] and the complexation of this reagent with chloro-benziodoxole **9** to form **9·10** is found to be 7.7 kcal/mol more stable than the separate species. In this complex, the Ag ion interacts with the Cl center of **9** with a distance of 2.53 Å, while the SCF_3 group is arranged parallel to the benziodoxole ring. In what follows, the subscript

https://dx.doi.org/10.1021/acs.joc.0c02306
J. Org. Chem. 2020, 85, 15577−15585

Scheme 4. Proposed Mechanism of the Synthesis of Benziodoxole-Based SCF_3 Transfer Reagent 7 as Obtained from the Current DFT Calculations

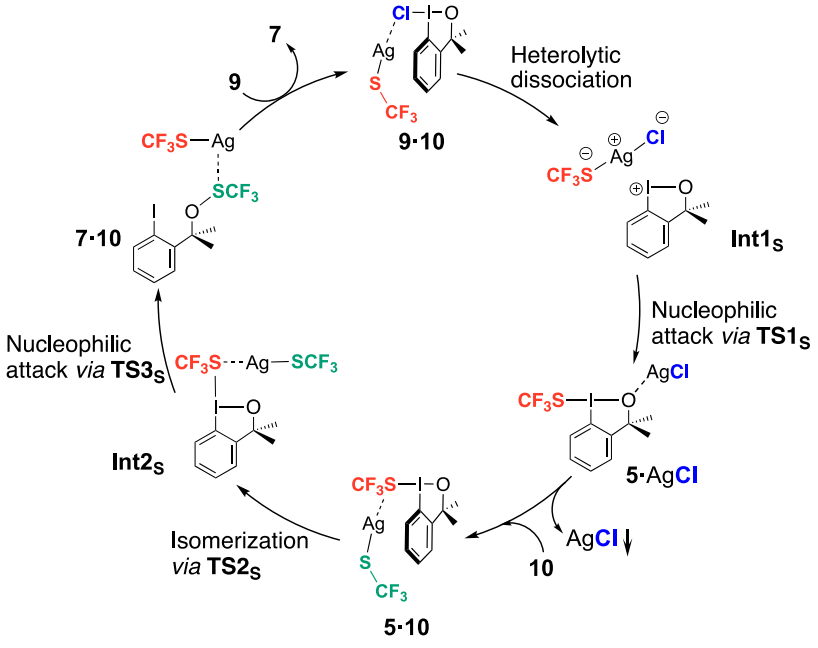

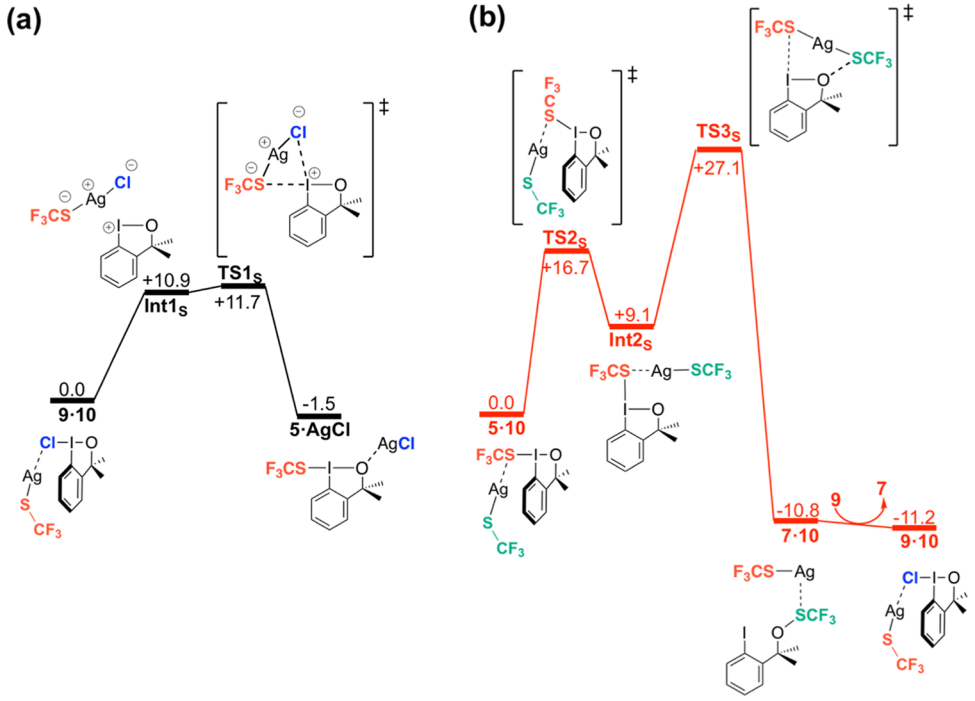

Figure 3. Calculated free energy profiles (kcal/mol) for the synthesis of the benziodoxole-based SCF_3 transfer reagent **7**. (a) Initial formation of the hypervalent iodine form **5**. (b) Conversion of **5** into the thioperoxide form **7**. Note that the energy associated with the precipitation of AgCl is not considered, and complex **5·10** is taken as the starting point of the second part of the reaction in (b).

"**S**" will be used in the names of the TSs and intermediates of this reaction to distinguish them from the ones involved in the synthesis of the Togni reagent discussed above.

Starting from complex **9·10**, the energetically most favorable pathway obtained by the calculations is shown in Scheme 4, with the associated energy profile given in Figure 3 and selected optimized geometries in Figure 4. In the first step, the silver ion in $AgSCF_3$ abstracts the chloride from **9** to yield an ion-pair intermediate **Int1$_S$** that is 10.9 kcal/mol higher in energy (Figure 3a). No transition state could be obtained for the formation of **Int1$_S$**, and the energy of the ion pair can be considered as a good approximation of the barrier.[24]

At **Int1$_S$**, the SCF_3 group can then readily transfer to the iodine through **TS1$_S$** to yield **5**, the hypervalent form of the reagent, in complex with AgCl (**5·AgCl** in Figure 3a). The barrier for this is very low, only 0.8 kcal/mol higher than **Int1$_S$**, i.e., 11.7 kcal/mol relative to **9·10**. At this stage, AgCl is expected to precipitate fully or partially, making the process **9·10→5**

https://dx.doi.org/10.1021/acs.joc.0c02306
J. Org. Chem. 2020, 85, 15577−15585

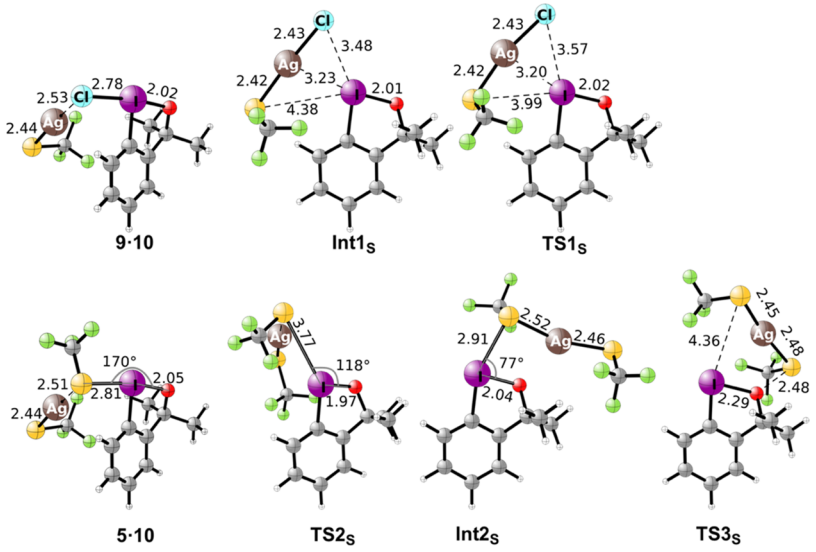

Figure 4. Optimized geometries of relevant transition states and intermediates involved in the synthesis of the benziodoxole-based SCF_3 transfer reagent 7.

irreversible, although the **5·AgCl** complex is only 1.5 kcal/mol lower than the starting complex **9·10** (Figure 3a).

The calculations thus show that the reaction leading to **5**, the hypervalent form of the reagent, takes place with a low barrier. How is then the thermodynamically more stable thioperoxide form **7** obtained? As established previously, the direct **5**→**7** isomerization is associated with prohibitively high barriers and can be ruled out (see the Supporting Information).[15,20] We have also considered the possibility of the direct formation of **7** by transfer of the SCF_3 group to the oxygen at either complex **9·10** or intermediate $\mathbf{Int1_S}$. The calculations show that the barriers for these scenarios are high, 25.3 and 27.8 kcal/mol, respectively, which are much higher than the energy of $\mathbf{TS1_S}$ (see the Supporting Information for details).

Instead, we found that the presence of the $AgSCF_3$ reagent **10** in the solution can catalyze the **5**→**7** isomerization with a reasonable barrier. Namely, another $AgSCF_3$ reagent can enter the cycle to form complex **5·10** with the hypervalent benziodoxole-SCF_3 **5**. Then, a trans−cis isomerization of the F_3CS−I−O bond takes place through $\mathbf{TS2_S}$, with a barrier of 16.7 kcal/mol, yielding $\mathbf{Int2_S}$, which is 9.1 kcal/mol higher in energy than **5·10**. The silver ion acts here as a Lewis acid, facilitating the *trans*−*cis* isomerization, a mode of action that has been observed in a number of metal-catalyzed reactions involving hypervalent iodine reagents.[25−29]

Next, the formation of complex **7·10** occurs through a five-membered S_N2-type transition state ($\mathbf{TS3_S}$), in which a nucleophilic attack of the SCF_3 of **10** takes place on the oxygen center concertedly with the dissociation of the I−O and I−SCF_3 bonds (Figure 4). This step has an overall barrier of 27.1 kcal/mol relative to **5·10**, which can be compared to the barrier of 36.7 kcal/mol calculated for the direct uncatalyzed isomerization from **5** to **7** (see the Supporting Information). The cycle closes by an exchange of **7** by **9** to regenerate **9·10**, and this step is calculated to be exergonic by 0.4 kcal/mol. It should be mentioned that we also found a plausible pathway from **5** to **7** involving the silver ion of AgCl, if one assumes that it does not precipitate in the solution (see the Supporting Information for details).

The calculations thus show that the hypervalent iodine form of the reagent is formed initially, but the presence $AgSCF_3$ provides a path to the thermodynamically more stable thioperoxide form **7**. However, although the obtained barrier of 27.1 kcal/mol is energetically viable under the reaction conditions of the experiments, it is rather high, which indicates that it might be possible to isolate **5** by running the reaction at low temperatures.

Very recently, Zhang and co-workers succeeded in the synthesis of the hypervalent trifluoromethylthio iodine reagent **12** by modifying the benziodoxole ring in **9** into an N-acetylbenziodazole one (**13** in Scheme 5).[30] Although the experimental procedure to synthesize **12** is very similar to the one used for **7**, the hypervalent (I−SCF_3) product could be obtained. We have also considered this reaction by calculations and found that the formation follows the same mechanism described above for **7**. That is, a heterolytic dissociation of the Cl−I bond in **13** takes place first, followed by a nucleophilic attack of SCF_3 at the iodine. Very importantly, however, the transformation of both **12** and **13** into the sulfenamide isomer **14** was found to be associated with very high barriers (>35 kcal/mol). Energy profiles and optimized geometries are given in the Supporting Information. These results thus demonstrate that the further isomerization of **12** is kinetically blocked, similarly to the Togni case, but in contrast to the situation with **5** that can convert to **7** with a reasonable barrier. The higher energy barrier in the case of **12** can be ascribed to the resonance effect of the acetyl substituent. Accordingly, when the acetyl group in **12** was replaced by a methyl in the calculations, the energy barrier for

Scheme 5. Synthesis of Zhang's Reagent 12 and Blocked Pathways for the Formation of the Sulfonamide 14

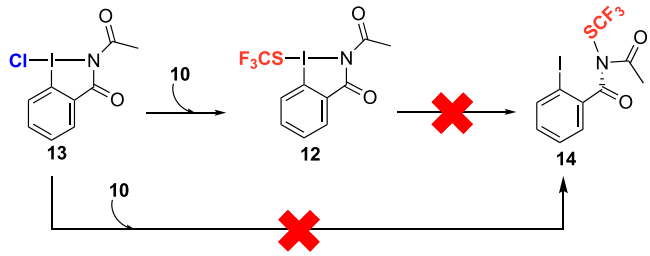

https://dx.doi.org/10.1021/acs.joc.0c02306
J. Org. Chem. 2020, 85, 15577−15585

the isomerization to the analogue of **14** decreased by as much as 10.7 kcal/mol (see the Supporting Information).

3. CONCLUSIONS

We have in the present work employed the DFT methodology to unravel the reaction mechanisms for the formation of the benziodoxole-based CF_3 (**1**) and SCF_3 (**7**) reagents. The calculations show that the two reactions follow quite different mechanisms, as shown in Schemes 3 and 4.

In the case of the synthesis of **1**, the mechanism involves the following steps: (i) nucleophilic attack by the fluorine of KF on the silicon center of the Ruppert−Prakash reagent **8** to generate a hypervalent silicon intermediate; (ii) heterolytic dissociation of the Si−CF_3 bond to yield the $(CH_3)_3SiF$ side product and a CF_3 carbanion stabilized by the potassium cation; and (iii) nucleophilic attack of the CF_3^- at iodine of fluoro-benziodoxole **2** to obtain the hypervalent iodine Togni reagent.

The calculations show that KF acts as a catalyst in this reaction, first donating a fluorine to activate **8** and generate CF_3^- and later receiving a fluorine back from the fluoro-benziodoxole reagent **2** (Scheme 3). The calculations further show that the pathways leading to the thermodynamically stable ether form of the reagent, i.e., compound **6**, are associated with high barriers, rationalizing the kinetic stability of the hypervalent iodine form **1**.

In the case of the thioperoxide SCF_3 reagent, the mechanism suggested by the calculations comprises an initial step in which the silver ion of the $AgSCF_3$ reagent **10** assists the heterolytic dissociation of the Cl−I bond of the chloro-benziodoxole **9**, generating an ion-pair intermediate. The SCF_3 group then transfers to the iodine to yield the hypervalent iodine form of the reagent (**5**). The barrier for the isomerization of **5** to the thermodynamically more stable thioperoxide isomer **7** was found to be energetically feasibly. The isomerization is catalyzed by the silver ion of the $AgSCF_3$ reagent **10**, and the mechanism involves a trans−cis isomerization of the F_3CS−I−O bond, followed by a transfer of the SCF_3 moiety from **10** to the oxygen center concomitantly with the dissociation of the I−O and I−SCF_3 bonds (Figure 4). The silver-catalyzed **5**→**7** isomerization has a ca. 10 kcal/mol lower energy barrier compared to the direct uncatalyzed isomerization. Interestingly, in the case of the synthesis of Zhang's reagent **12**, the catalytic power of the silver ion is not sufficient to catalyze the isomerization, and the hypervalent form can thus be achieved. In this case, the high energy barrier could be attributed to the acetyl substituent of the reagent.

We hope that the mechanistic insights offered by the current calculations will provide a basis for the rational development of revised protocols for the synthesis of new kinds of hypervalent iodine fluorine transfer reagents.

4. COMPUTATIONAL DETAILS

The B3LYP-D3(BJ) functional, i.e., the B3LYP functional[31,32] including the D3 dispersion correction with the Becke−Johnson damping function,[33,34] was used for all calculations presented in this work. The Gaussian 09 package was employed.[35] Geometry optimizations were carried out with a medium-sized mixed basis set consisting of LANL2DZ for K and Ag, LANL2DZpd for I, and 6-31G(d,p) for the other atoms. The geometries were optimized including implicit solvation using the SMD method.[36] Following the experimental conditions, acetonitrile (ε = 35.69) was used in the study of the synthesis of the Togni reagent **1** (reaction I)[9] and tetrahydrofuran (ε = 7.43) for the formation of **7** (reaction II).[13]

Vibrational frequencies were calculated at the same level of theory as the geometry optimization, and the Gibbs free energy corrections were calculated using the quasi-rigid-rotor-harmonic-oscillator (qRRHO) approximation at room temperature.[37] Experimentally, the reactions were performed at 263 and 323 K for reactions I and II, respectively.[9,13] The effect of using the experimental temperatures in the calculations was found to be small, as discussed in the Supporting Information.

Standard state corrections were added to account for the conversion from the 1 atm ideal gas to the 1 M standard state of the solutes and 19.1 M for the acetonitrile solvent. This implies that the term $RT \ln(24.5)$ = +1.9 kcal/mol was added to the energies of all complexes, except for the acetonitrile (in the case where it was considered explicitly, see above) for which the value $RT \ln(24.5 \times 19.1)$ = +3.6 kcal/mol was added.

To improve the accuracy of the electronic structure calculations, single-point gas-phase energies using a larger basis set consisting of LANL2DZ for K and Ag, LANL2DZpd for I, and 6-311+G(2d,2p) for the other atoms were calculated on the basis of the optimized geometries. The final energies reported in the paper are thus these large basis set gas-phase energies corrected for Gibbs free energy, standard state change, and solvation, where the latter was calculated by comparing the energies obtained from the geometry optimization with the gas-phase values calculated with the same basis set.

■ ASSOCIATED CONTENT

Supporting Information

The Supporting Information is available free of charge at https://pubs.acs.org/doi/10.1021/acs.joc.0c02306.

Additional results discussed in the text; absolute energies and energy corrections; and Cartesian coordinates (PDF)

■ AUTHOR INFORMATION

Corresponding Authors

Kalman J. Szabo − *Department of Organic Chemistry, Arrhenius Laboratory, Stockholm University, SE-106 91 Stockholm, Sweden;* orcid.org/0000-0002-9349-7137; Email: kalman.j.szabo@su.se

Fahmi Himo − *Department of Organic Chemistry, Arrhenius Laboratory, Stockholm University, SE-106 91 Stockholm, Sweden;* orcid.org/0000-0002-1012-5611; Email: fahmi.himo@su.se

Author

Oriana Brea − *Department of Organic Chemistry, Arrhenius Laboratory, Stockholm University, SE-106 91 Stockholm, Sweden*

Complete contact information is available at: https://pubs.acs.org/10.1021/acs.joc.0c02306

Notes

The authors declare no competing financial interest.

■ ACKNOWLEDGMENTS

The authors thank the Knut and Alice Wallenberg Foundation (Dnr: 2018.0066) and the Swedish Research Council for financial support.

REFERENCES

(1) Zhu, Y.; Han, J.; Wang, J.; Shibata, N.; Sodeoka, M.; Soloshonok, V. A.; Coelho, J. A. S.; Toste, F. D. Modern Approaches for Asymmetric Construction of Carbon−Fluorine Quaternary Stereogenic Centers: Synthetic Challenges and Pharmaceutical Needs. *Chem. Rev.* **2018**, *118*, 3887−3964.

(2) Jeschke, P. The Unique Role of Fluorine in the Design of Active Ingredients for Modern Crop Protection. *ChemBioChem* **2004**, *5*, 570−589.

(3) Preshlock, S.; Tredwell, M.; Gouverneur, V. 18F-Labeling of Arenes and Heteroarenes for Applications in Positron Emission Tomography. *Chem. Rev.* **2016**, *116*, 719−766.

(4) Mei, H.; Han, J.; Fustero, S.; Medio-Simon, M.; Sedgwick, D. M.; Santi, C.; Ruzziconi, R.; Soloshonok, V. A. Fluorine-Containing Drugs Approved by the FDA in 2018. *Chem. − Eur. J.* **2019**, *25*, 11797−11819.

(5) Charpentier, J.; Früh, N.; Togni, A. Electrophilic Trifluoromethylation by Use of Hypervalent Iodine Reagents. *Chem. Rev.* **2015**, *115*, 650−682.

(6) Liang, T.; Neumann, C. N.; Ritter, T. Introduction of Fluorine and Fluorine-Containing Functional Groups. *Angew. Chem., Int. Ed.* **2013**, *52*, 8214−8264.

(7) Eisenberger, P.; Gischig, S.; Togni, A. Novel 10-I-3 Hypervalent Iodine-Based Compounds for Electrophilic Trifluoromethylation. *Chem. − Eur. J.* **2006**, *12*, 2579−2586.

(8) Legault, C. Y.; Prévost, J. 1-Fluoro-3,3-Dimethyl-1,3-Dihydro-1λ(3)-Benzo[d][1,2]Iodoxole. *Acta Crystallogr., Sect. E* **2012**, *68*, o1238.

(9) Matoušek, V.; Pietrasiak, E.; Schwenk, R.; Togni, A. One-Pot Synthesis of Hypervalent Iodine Reagents for Electrophilic Trifluoromethylation. *J. Org. Chem.* **2013**, *78*, 6763−6768.

(10) Geary, G. C.; Hope, E. G.; Singh, K.; Stuart, A. M. Electrophilic Fluorination Using a Hypervalent Iodine Reagent Derived from Fluoride. *Chem. Commun.* **2013**, *49*, 9263−9265.

(11) Matoušek, V.; Václavík, J.; Hájek, P.; Charpentier, J.; Blastik, Z. E.; Pietrasiak, E.; Budinská, A.; Togni, A.; Beier, P. Expanding the Scope of Hypervalent Iodine Reagents for Perfluoroalkylation: From Trifluoromethyl to Functionalized Perfluoroethyl. *Chem. − Eur. J.* **2016**, *22*, 417−424.

(12) Zhang, W.; Zhu, J.; Hu, J. Electrophilic (Phenylsulfonyl)-Difluoromethylation of Thiols with a Hypervalent Iodine(III)−CF_2SO_2Ph Reagent. *Tetrahedron Lett.* **2008**, *49*, 5006−5008.

(13) Shao, X.; Wang, X.; Yang, T.; Lu, L.; Shen, Q. An Electrophilic Hypervalent Iodine Reagent for Trifluoromethylthiolation. *Angew. Chem., Int. Ed.* **2013**, *52*, 3457−3460.

(14) Vinogradova, E. V.; Müller, P.; Buchwald, S. L. Structural Reevaluation of the Electrophilic Hypervalent Iodine Reagent for Trifluoromethylthiolation Supported by the Crystalline Sponge Method for X-Ray Analysis. *Angew. Chem., Int. Ed.* **2014**, *53*, 3125−3128.

(15) Sun, T.-Y.; Wang, X.; Geng, H.; Xie, Y.; Wu, Y.-D.; Zhang, X.; Schaefer, H. F., III Why Does Togni's Reagent I Exist in the High-Energy Hypervalent Iodine Form? Re-Evaluation of Benziodoxole Based Hypervalent Iodine Reagents. *Chem. Commun.* **2016**, *52*, 5371−5374.

(16) The mechanism discussed for the formation of **Int2** (Figure 1) considers that the nucleophilic attack via **TS1** takes place from the backside of the Si-SCF_3 bond in **6**. The generated hypervalent bond in **Int1** is between F-Si-CF_3. The nucleophilic attack can also occur from the frontside of the Si-SCF_3 bond in **8**, forming instead a CH_3-Si-CF_3 hypervalent bond. The two pathways are compared in the Supporting Information.

(17) Luo, G.; Luo, Y.; Qu, J. Direct Nucleophilic Trifluoromethylation Using Fluoroform: A Theoretical Mechanistic Investigation and Insight into the Effect of Alkali Metal Cations. *New J. Chem.* **2013**, *37*, 3274−3280.

(18) Burton, D. J.; Wiemers, D. M. A Remarkably Simple Preparation of (Trifluoromethyl)Cadmium and -Zinc Reagents Directly from Difluorodihalomethanes. *J. Am. Chem. Soc.* **1985**, *107*, 5014−5015.

(19) Pu, M.; Sanhueza, I. A.; Senol, E.; Schoenebeck, F. Divergent Reactivity of Stannane and Silane in the Trifluoromethylation of PdII: Cyclic Transition State versus Difluorocarbene Release. *Angew. Chem., Int. Ed.* **2018**, *57*, 15081−15085.

(20) Koichi, S.; Leuthold, B.; Lüthi, H. P. Why Do the Togni Reagent and Some of Its Derivatives Exist in the High-Energy Hypervalent Iodine Form? New Insight into the Origins of Their Kinetic Stability. *Phys. Chem. Chem. Phys.* **2017**, *19*, 32179−32183.

(21) Adams, D. J.; Clark, J. H.; Hansen, L. B.; Sanders, V. C.; Tavener, S. J. Reaction of Tetramethylammonium Fluoride with Trifluoromethyltrimethylsilane. *J. Fluorine Chem.* **1998**, *92*, 123−125.

(22) Kolomeitsev, A.; Movchun, V.; Rusanov, E.; Bissky, G.; Lork, E.; Röschenthaler, G.-V.; Kirsch, P. Different Fluoride Anion Sources and (Trifluoromethyl)Trimethylsilane: Molecular Structure of Tris-(Dimethylamino)Sulfonium Bis(Trifluoromethyl)Trimethylsiliconate, the First Isolated Pentacoordinate Silicon Species with Five Si−C Bonds. *Chem. Commun.* **1999**, *11*, 1017−1018.

(23) For comparison, **TS3** was recalculated in the presence of one explicit acetonitrile solvent molecule. The effect was found to be small, see Supporting Information for details.

(24) The infinitely separated ions are calculated to be 15.8 kcal/mol higher than complex **9·10**.

(25) Jobin-Des Lauriers, A.; Legault, C. Y. Metathetical Redox Reaction of (Diacetoxyiodo)Arenes and Iodoarenes. *Molecules* **2015**, *20*, 22635−22644.

(26) Izquierdo, S.; Essafi, S.; del Rosal, I.; Vidossich, P.; Pleixats, R.; Vallribera, A.; Ujaque, G.; Lledós, A.; Shafir, A. Acid Activation in Phenyliodine Dicarboxylates: Direct Observation, Structures, and Implications. *J. Am. Chem. Soc.* **2016**, *138*, 12747−12750.

(27) Zhou, B.; Yan, T.; Xue, X.-S.; Cheng, J.-P. Mechanism of Silver-Mediated Geminal Difluorination of Styrenes with a Fluoroiodane Reagent: Insights into Lewis-Acid-Activation Model. *Org. Lett.* **2016**, *18*, 6128−6131.

(28) Zhang, J.; Szabó, K. J.; Himo, F. Metathesis Mechanism of Zinc-Catalyzed Fluorination of Alkenes with Hypervalent Fluoroiodine. *ACS Catal.* **2017**, *7*, 1093−1100.

(29) Mai, B. K.; Szabó, K. J.; Himo, F. Mechanisms of Rh-Catalyzed Oxyfluorination and Oxytrifluoromethylation of Diazocarbonyl Compounds with Hypervalent Fluoroiodine. *ACS Catal.* **2018**, *8*, 4483−4492.

(30) Yang, X.-G.; Zheng, K.; Zhang, C. Electrophilic Hypervalent Trifluoromethylthio-Iodine(III) Reagent. *Org. Lett.* **2020**, *22*, 2026−2031.

(31) Becke, A. D. Density-Functional Exchange-Energy Approximation with Correct Asymptotic Behavior. *Phys. Rev. A* **1988**, *38*, No. 3098.

(32) Becke, A. D. Density-functional Thermochemistry. III. The Role of Exact Exchange. *J. Chem. Phys.* **1993**, *98*, 5648−5652.

(33) Grimme, S.; Antony, J.; Ehrlich, S.; Krieg, H. A Consistent and Accurate Ab Initio Parametrization of Density Functional Dispersion Correction (DFT-D) for the 94 Elements H-Pu. *J. Chem. Phys.* **2010**, *132*, No. 154104.

(34) Grimme, S.; Ehrlich, S.; Goerigk, L. Effect of the Damping Function in Dispersion Corrected Density Functional Theory. *J. Comput. Chem.* **2011**, *32*, 1456−1465.

(35) Frisch, M. J.; Trucks, G. W.; Schlegel, H. B.; Scuseria, G. E.; Robb, M. A.; Cheeseman, J. R.; Scalmani, G.; Barone, V.; Petersson, G. A.; Nakatsuji, H.; Li, X.; Caricato, M.; Marenich, A. V.; Bloino, J.; Janesko, B. G.; Gomperts, R.; Mennucci, B.; Hratchian, H. P.; Ortiz, J. V.; Izmaylov, A. F.; Sonnenberg, J. L.; Williams Ding, F.; Lipparini, F.; Egidi, F.; Goings, J.; Peng, B.; Petrone, A.; Henderson, T.; Ranasinghe, D.; Zakrzewski, V. G.; Gao, J.; Rega, N.; Zheng, G.; Liang, W.; Hada, M.; Ehara, M.; Toyota, K.; Fukuda, R.; Hasegawa, J.; Ishida, M.; Nakajima, T.; Honda, Y.; Kitao, O.; Nakai, H.; Vreven, T.; Throssell, K.; Montgomery, J. A., Jr.; Peralta, J. E.; Ogliaro, F.; Bearpark, M. J.; Heyd, J. J.; Brothers, E. N.; Kudin, K. N.; Staroverov, V. N.; Keith, T. A.; Kobayashi, R.; Normand, J.; Raghavachari, K.; Rendell, A. P.; Burant, J. C.; Iyengar, S. S.; Tomasi, J.; Cossi, M.; Millam, J. M.; Klene, M.; Adamo, C.; Cammi, R.; Ochterski, J. W.; Martin, R. L.; Morokuma, K.;

https://dx.doi.org/10.1021/acs.joc.0c02306
J. Org. Chem. 2020, 85, 15577−15585

Farkas, O.; Foresman, J. B.; Fox, D. J. *Gaussian 09*, revision D.01; Gaussian, Inc.: Wallingford, CT, 2019.
(36) Marenich, A. V.; Cramer, C. J.; Truhlar, D. G. Universal Solvation Model Based on Solute Electron Density and on a Continuum Model of the Solvent Defined by the Bulk Dielectric Constant and Atomic Surface Tensions. *J. Phys. Chem. B* **2009**, *113*, 6378−6396.
(37) Grimme, S. Supramolecular Binding Thermodynamics by Dispersion-Corrected Density Functional Theory. *Chem. − Eur. J.* **2012**, *18*, 9955−9964.

https://dx.doi.org/10.1021/acs.joc.0c02306
J. Org. Chem. 2020, 85, 15577−15585